X-ray structure of *Galdieria* Rubisco complexed with one sulfate ion per active site

Yousuke Okano[a], Eiichi Mizohata[a], Yong Xie[a], Hiroyoshi Matsumura[a], Hajime Sugawara[a,1], Tsuyoshi Inoue[a], Akiho Yokota[b,c], Yasushi Kai[a,*]

[a] *Department of Materials Chemistry, Graduate School of Engineering, Osaka University, 2-1 Yamada-oka, Suita, Osaka 565-0871, Japan*
[b] *Graduate School of Biological Sciences, Nara Institute of Science and Technology (NAIST), 8916-5 Takayama, Ikoma, Nara 630-0101, Japan*
[c] *Plant Molecular Physiology Laboratory, Research Institute of Innovative Technology for the Earth (RITE), 9-2 Kizugawadai, Kizu-cho, Soraku-gun, Kyoto 619-0292, Japan*

Received 24 June 2002; accepted 17 July 2002

First published online 13 August 2002

Edited by Marc Van Montague

Abstract Ribulose-1,5-bisphosphate carboxylase/oxygenase (Rubisco) catalyzes the reactions of carboxylation and oxygenation of ribulose-1,5-bisphosphate. These reactions require that the active site should be closed by a flexible loop (loop 6) of the large subunit. Rubisco from a red alga, *Galdieria partita*, has the highest specificity for carboxylation reaction among the Rubiscos hitherto reported. The crystal structure of unactivated *Galdieria* Rubisco has been determined at 2.6 Å resolution. The electron density map reveals that a sulfate binds only to the P1 anion-binding site of the active site and the loop 6 is closed. *Galdieria* Rubisco has a unique hydrogen bond between the main chain oxygen of Val332 on the loop 6 and the ε-amino group of Gln386 of the same large subunit. This interaction is likely to be crucial to understanding for stabilizing the loop 6 in the closed state and to making a higher affinity for anionic ligands. **© 2002 Federation of European Biochemical Societies. Published by Elsevier Science B.V. All rights reserved.**

Key words: X-ray crystallography; Photosynthesis; Ribulose-1,5-bisphosphate carboxylase/oxygenase; SO_4^{2-}-bound form; α/β barrel

1. Introduction

Ribulose-1,5-bisphosphate carboxylase/oxygenase (Rubisco; EC 4.1.1.39) catalyzes two separate reactions, carboxylation and oxygenation reactions. The gaseous CO_2 and O_2 are the competitive substrates in Rubisco, the activity of which is characterized by the specificity factor, $S_{c/o}$ ($= V_cK_o/V_oK_c$, where V_c, V_o and K_c, K_o are the V_{max} and K_m values for CO_2 and O_2, respectively). A thermophilic red alga, Rubisco from *Galdieria partita* has the highest $S_{c/o}$ (364 and 238 at 15 and 25°C, respectively) among the Rubiscos reported so far [1].

Structural analyses of Rubiscos from higher plants, green and red algae, a cyanobacterium, photosynthetic bacteria, and an archaebacterium have been reported [2–4,12–24]. Rubiscos from most of photosynthetic organisms are composed of eight large and eight small subunits (L_8S_8). These enzymes have an α/β barrel domain in the large subunit. The active site is on the large subunit and consists of P1 and P2 anion-binding sites and the metal-binding site [2]. The active site must be covered by a flexible loop 6 during carboxylation reaction. The residues 328–339 in the loop 6 are completely conserved among all the L_8S_8 Rubiscos. The previous report described that P1 and P2 sites consist of four subsites (proximal subsite, distal subsite, etc.) [2]. The distance between P1 and P2 sites correlates to open and closed states of the active site. The active site shows a closed state when the distance between two anions in P1 and P2 sites is the shortest. The anion positions are named P1α and P2α positions in this paper. On the other hand, the open structure shows the long distance between P1 and P2 sites; named P1β and P2β positions.

The loop 6 plays a vital role in covering the active site and in catalyzing the carboxylation reaction. Lys^L334 (superscript ^{L} stands for the residue in the large subunit), located in the middle of the loop 6, interacts with C-2 carboxylate group of the carboxylation reaction intermediate (3-keto-2CABP) and the side chain of Glu^L60 from the other large subunit in an L_2 dimer [3]. The loop 6-deleted mutant enolizes ribulose-1,5-bisphosphate (RuBP), but cannot process 3-keto-2CABP into the product [3]. The structural changes in both Val^L332 and Asp^L338 donate the loop 6 and result in open and closed states.

Several structures of Rubisco complexed with substrate analogues, inhibitors, and reaction products have been determined by X-ray crystallography, while these structures were distributed between open and closed state in the active site [2,3]. Rubiscos complexed with 2-CABP (Mg^{2+}-activated), 4-CABP (metal-free) and XuBP (metal-free) take the closed state formed by the loop 6, whereas Rubiscos complexed with 3-PGA (Mg^{2+}-activated), 2-CABP (metal-free), PO_4^{3-} (metal-free) and SO_4^{2-} (metal-free) take open state (Table 1).

In these closed structures of L_8S_8 Rubiscos hitherto reported indicate the anion-binding sites adopt the P1α and P2α structure [2].

*Corresponding author. Fax: (81)-6-6879 7409.
E-mail address: kai@chem.eng.osaka-u.ac.jp (Y. Kai).

[1] Present address: Metabolic Function Research Group, RIKEN Plant Science Center, Hirosawa 2-1, Wako, Saitama 351-0198, Japan.

Abbreviations: 2-CABP, 2-carboxyarabinitol-1,5-bisphosphate; 3-PGA, 3-phosphoglycerate; HEPES, *N*-2-hydroxyethylpiperazine-*N*′-2-ethanesulfonic acid; K_c, Michaelis constant for CO_2; K_o, Michaelis constant for O_2; L_8S_8, eight large and eight small subunits; PDB, Protein Data Bank; Rubisco, ribulose-1,5-bisphosphate carboxylase/oxygenase; RuBP, ribulose-1,5-bisphosphate; $S_{c/o}$, specificity factor; V_c, maximum velocity of carboxylation; V_o, maximum velocity of oxygenation

0014-5793/02/$22.00 © 2002 Federation of European Biochemical Societies. Published by Elsevier Science B.V. All rights reserved.
PII: S0014-5793(02)03148-4

Table 1
Crystal structures of L_8S_8 Rubiscos

Source	Metal ion	Ligand	Anion position	Active site	Res. (Å)	PDB ID
Spinach	Mg^{2+}	2-CABP	P1α, P2α	closed	1.6	8RUC [18]
Spinach	Mg^{2+}	2-CABP	P1α, P2α	closed	1.8	1BUR [17]
Spinach	Mg^{2+}	–	–	open	2.2	1AUS [20]
Spinach	Ca^{2+}	RuBP	P1β, P2β	open	2.2	1RXO [21]
Spinach	Mg^{2+}	3-PGA	P1β, P2β	open	2.2	1AA1 [20]
Spinach	–	4-CABP	P1α, P2α	closed	2.3	1RBO [19]
Spinach	–	2,2-diol-XuBP	P1α, P2α	closed	2.3	1RCO [19]
Spinach	–	RuBP	P1α, P2α	closed	2.4	1RCX [21]
Tobacco	–	SO_4^{2-}/PO_4^{3-}	P1β, P2β	open	2.0	3RUB [12]
Tobacco	–	PO_4^{3-}	P1β, P2β	open	2.45	1EJ7 [2]
Tobacco	–	2-CABP	P1β, P2β	open	2.7	1RLC [15]
Tobacco	–	–	–	open	2.5	1RLD [13]
Tobacco	Mg^{2+}	2-CABP	P1α, P2α	closed	2.7	4RUB [12]
C. reinhardtii	Mg^{2+}	2-CABP	P1α, P2α	closed	1.4	1GK8 [23]
C. reinhardtii	Mg^{2+}	2-CABP	P1α, P2α	closed	1.84	1IR2 [24]
G. partita	Mg^{2+}	2-CABP	P1α, P2α	closed	2.4	1BWV [4]
G. partita	–	SO_4^{2-}	P1α	closed	2.6	–
Alcaligenes eutrophus	–	PO_4^{3-}	P1β, P2β	open	2.7	1BXN [22]
Synechococcus	Mg^{2+}	2-CABP	P1α, P2α	closed	2.2	1RBL [16]
Synechococcus	–	XuBP	P1α, P2α	closed	2.3	1RSC [14]

The X-ray crystal structure of *Galdieria* Rubisco displays that P1α is occupied by a sulfate, and the loop 6 covers the active site without any substrate analogue. Here we discuss that the loop 6 in *Galdieria* Rubisco has a unique hydrogen bond contributing to close the active site, resulting in the highest affinity for CO_2.

2. Materials and methods

2.1. Purification and crystallization

Galdieria was cultured as previously described [1]. Rubisco was purified at 0–4°C. The cells suspended in extraction buffer (50 mM HEPES–KOH, pH 7.6, 1 mM EDTA, 1 mM dithiothreitol, 1 mM PMSF, 10 μM leupeptin) were disintegrated by using a bead beater. The crude extract was centrifuged at 15 000×*g* for 20 min, and the supernatant was collected. A fraction that precipitated between 30 and 60% ammonium sulfate was centrifuged at 15 000×*g* for 20 min. The precipitate was dissolved in elution buffer (50 mM HEPES–KOH, pH 7.6, 1mM EDTA, 1 mM dithiothreitol) containing 30% ammonium sulfate. The sample was applied to a column of butyl-Toyopearl (Tosoh, Tokyo, Japan) and eluted with a 30–0% ammonium sulfate gradient in the elution buffer. The active fractions were pooled, applied to a HiLoad 26/60 Superdex 200 prep grade column (Amersham Pharmacia Biotech, Tokyo, Japan), and developed with the elution buffer. Finally, the active fractions were pooled and used for crystallization.

Crystals were grown at 20°C by the hanging-drop vapor-diffusion method. The purified Rubisco was concentrated to 22.7 mg/ml. Drops consisted of 3 μl of Rubisco solution with an equal volume of well liquor (100 mM HEPES–NaOH, pH 7.5, 12% (w/v) polyethylene glycol 4000, 5% (w/v) 2-methyl-2,4-pentanediol, and 20% (w/v) glycerol). In 7 days, the typical size of crystals grew to 0.1×0.1×0.05 mm. Crystals belonged to the monoclinic space group of *C*2 with cell constants of $a = 201.3$, $b = 146.9$, $c = 197.2$ Å, $\beta = 99.8°$.

2.2. Data collection, structure determination and refinement

X-ray diffraction intensities were measured at beamline BL18B of the Photon Factory (PF), High Energy Acceleration Research Organization, Tsukuba, Japan. Diffraction data were processed with the programs *DPS* [6] and *SCALA* [7]. The structure was determined by the molecular replacement method using the program *AMoRe* [8]. A crystal structure of the complex of activated *Galdieria* Rubisco and 2-CABP (Protein Data Bank (PDB) ID, 1BWV [4]) was used as the search model. The asymmetric unit in this crystal was L_8S_8 and V_m [10] was 2.65 $Å^3$ Da^{-1}. Refinement was carried out using the program *CNS* [11] without non-crystallographic symmetry restraints/constraints. The structure was visualized and modified using the program *TURBO-FRODO* [9]. Data collection and refinement statistics are summarized in Table 2. The coordinates and structure factors have been deposited in the PDB with ID 1IWA.

3. Results and discussion

3.1. Overall structure

The final model of unactivated *Galdieria* Rubisco has been refined at 2.6 Å resolution. The root-mean-square deviation (RMSD) of the Cα-atoms between all the subunits of unactivated Rubisco and those of Rubisco complexed with 2-CABP are 0.22 Å. All the subunits of N-terminal domain and C-terminal strand are not different between unactivated Rubisco and those of Rubisco complexed with 2-CABP.

Unexpectedly, the higher peak of electron density is located in P1 site near the positively charged side chain of $Lys^{L}334$.

Table 2
Data collection and refinement statistics

Data collection	
X-ray source/detector system	PF (BL18B)/ADSC Quantum 4R [5]
Wavelength (Å)	1.0000
Space group	*C*2
Cell constants (Å, °)	$a = 201.3$, $b = 146.9$, $c = 197.2$, $\beta = 99.8$
Resolution range (Å	40.8–2.6 (2.76–2.6)
No. of measured/unique reflections	895 084/172 258
Completeness (%)	98.9 (97.4)
R_{merge}[a] (%)	10.3 (30.6)
Refinement	
Resolution range (Å)	40.0–2.6
No. of unique reflections	172 258
R_{cryst}[b] (%)/R_{free}[c] (%)	17.2/23.5
No. of non-hydrogen protein atoms	38 856
No. of water molecules	2 876
RMSD	
Bond lengths (Å)	0.006
Bond angles (°)	1.34

Values in parentheses refer to outermost shells: 2.76–2.6 Å resolution. RMSD, root-mean-square deviation.

[a] $R_{merge} = S_j S_h |I_{h,j} - \langle I_h \rangle| / S_j S_h \langle I_h \rangle$.

[b] $R_{cryst} = S||F_o| - |F_c|| / S|F_o|$ summed over only data (95%) used for refinement.

[c] $R_{free} = S||F_o| - |F_c|| / S|F_o|$ summed over only data (5%) set aside as the test set.

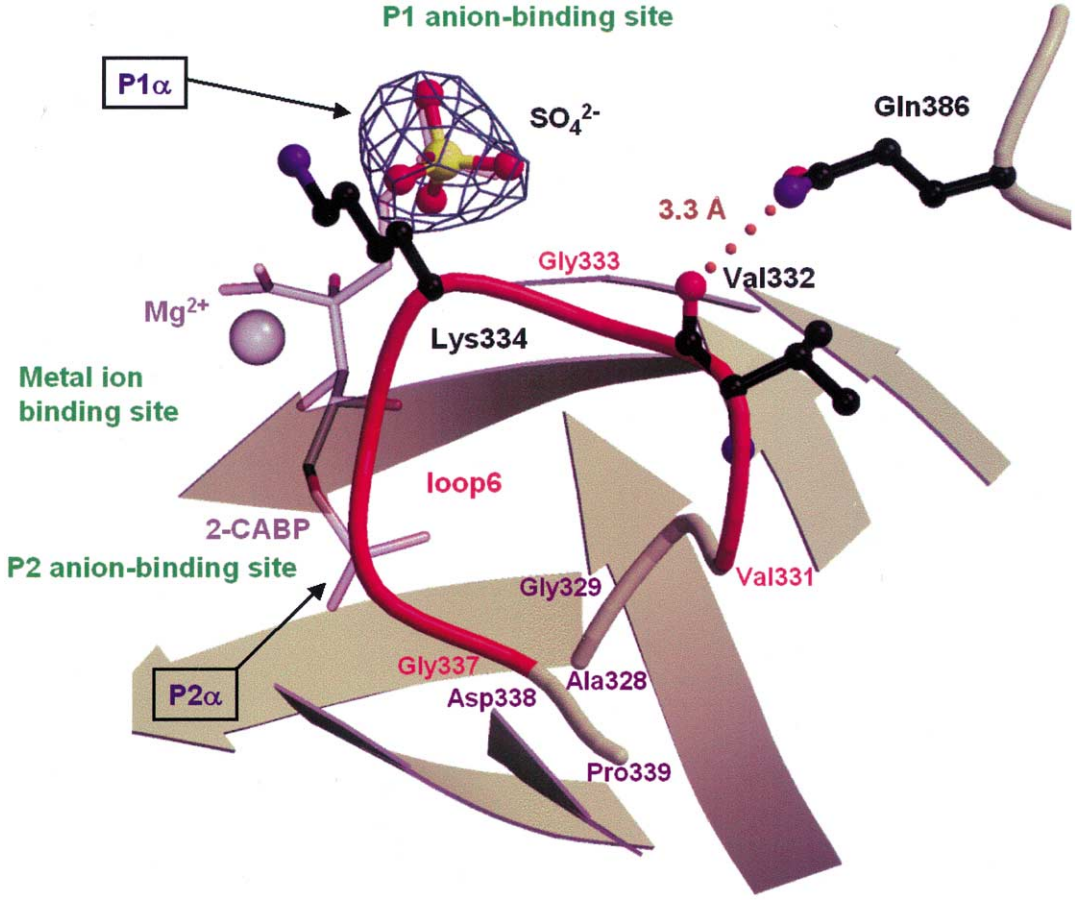

Fig. 1. Active site structure in Rubiscos structure of *Galdieria* metal-free Rubisco bound with SO_4^{2-}. Oxygen, nitrogen, and sulfur atoms are shown in red and purple and yellow. The metal ion and the bound 2-CABP of *Galdieria* Rubisco(1BWV) are shown with some transparency. The loop 6 of *Galdieria* is shown in red.

The electron density is large enough to accommodate a sulfate or phosphate. Although neither sulfate nor phosphate is included in the crystallization solution, ammonium sulfate was used in a purification step. Because the *B*-factors of sulfates are similar to that of the atoms around the binding site, we concluded that the electron density results from binding of a sulfate to the P1 site. When occupancies were set to 1, the average *B*-factors of sulfates among the eight large subunits were calculated at 58.5 Å^2. These values are same for the residues that bind the sulfates. The average *B*-factor and Wilson *B*-factor of this crystal structure are 27.9 Å^2 and 29.9 Å^2, respectively.

In the previous reports, unactivated Rubiscos complexed with sulfate or phosphate were in the open state structure (Table 1). Surprisingly, the loop 6 structure of unactivated *Galdieria* Rubisco is closed as that of *Galdieria* Rubisco complexed with 2-CABP (PDB ID, 1BWV).

3.2. Comparison between the novel open and closed structures

The electron density in the active site clearly indicates that the sulfate binds to α-subsite of the P1 site, and the active site is covered by the loop 6 (Fig. 1). The open structure of tobacco Rubisco (1EJ7) shows that two phosphates bind to the active site and two phosphates locate in P1β and P2β positions. Moreover, the occupancy of the phosphate in the P2β position is higher than that of the phosphate in the P1β position.

In our structure, the P2 site is not occupied by any anions; thereby the P2 site appears not to contribute to induce the closed state of loop 6 (Figs. 1 and 2). This observation is consistent to the idea that movement of the P1 phosphate plays a central role in triggering the active site closure [2].

In the present structure, the main chain oxygen of Val^{L}332 forms a hydrogen bond of 3.3 Å with the ε-amino group of Gln^{L}386. In *Galdieria* Rubisco complexed with 2-CABP (1BWV), the hydrogen bond is found between Val^{L}332 and Gln^{L}386 at the distance of 2.8 Å. In contrast, the high resolution structures of Rubiscos complexed with 2-CABP show that His^{L}386 is far from Val^{L}332, 3.9 Å in spinach (8RUC), 3.7 Å in *Synechococcus* (1RBL), and 3.7 Å in *Chlamydomonas reinhardtii* (1GK8 and 1IR2). Consequently, the latter of these Rubiscos have no hydrogen bond between Val^{L}332 and His^{L}386.

The K_c value of a *Galdieria* Rubisco is the smallest among those of other Rubiscos hitherto reported [1]. The previous study of Rubisco complexed with 2-CABP (1BWV) reported novel hydrogen bonds between the side chain of Glu^{L}336 and the main chain of Thr^{L}472, the main chain of Gly^{L}329 and the side chain of Tyr^{L}346 [4]; these have not been observed with other Rubiscos. The interactions may be responsible for the locking of the loop 6 on the active site. Moreover, these and the unique interaction between Val^{L}332 and Gln^{L}386 in *Galdieria* Rubisco strengthens the closed conformation of the loop 6 and promotes the interaction between Lys^{L}334 and the

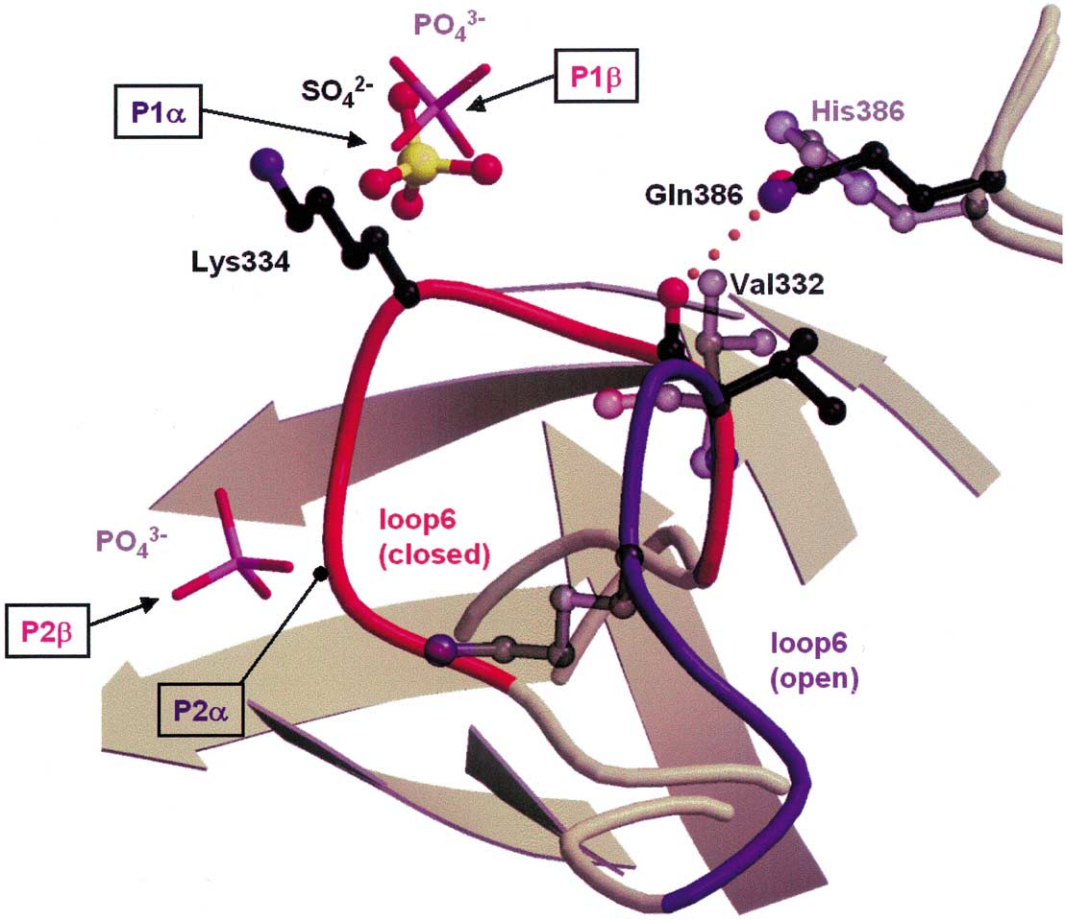

Fig. 2. The comparison in open/closed structure of the loop 6. The loop 6 structure of tobacco Rubisco (1EJ7) is shown in blue and that of *Galdieria* in shown red. This figure was drawn by the programs *MOLSCRIPT* and *RASTER3D*.

anion in P1α position. Thus, the stability of the loop 6 in the closed state may be related to the efficient CO_2 fixation of *Galdieria* Rubisco.

Acknowledgements: We thank Drs. M. Suzuki and N. Igarashi for kind help in the data collection at the PF. This work was supported by Grant-in-Aid for Scientific Research (A), No. 10305065, Ministry of Education, Culture, Sports, Science and Technology. This study was also supported by RAB/METI and by the 'Research for the Future' program (JSPS-RFTF97R16001) of the Japan Society of the Promotion of Science. Further, this study was supported by Structural Biology Sakabe Project (SBSP), Foundation for Advancement of International Science (FAIS).

References

[1] Uemura, K., Anwaruzzaman, Miyachi, S., Yokota, A. and Kai, Y. (1996) J. Biol. Chem. 271, 26449–46452.
[2] Duff, A.P., Andrews, T.J. and Curmi, P.M.G. (2000) J. Mol. Biol. 298, 903–916.
[3] Cleland, W.W., Andrews, T.J., Gutteridge, S., Hartman, F.C. and Lorimer, G.H. (1998) Chem. Rev. 98, 549–561.
[4] Sugawara, H., Yamamoto, H., Shibata, N., Inoue, T., Okada, S., Miyake, C., Yokota, A. and Kai, Y. (1999) J. Biol. Chem. 274, 15655–15661.
[5] Watanabe, N., Nakagawa, A., Adachi, S. and Sakabe, N. (1995) Rev. Sci. Instrum. 66, 1824–1826.
[6] Rossmann, M.G. and van Beek, C.G. (1999) Acta Cryst. D55, 1631–1640.
[7] Collaborative Computational Project, 1994. Acta Cryst. D50, 760–763
[8] Navaza, J. (1994) Acta Crystallogr. A50, 157–163.
[9] Roussel, A. Inisan, A.G. and Cambillau, C. (1996) AFMB and BioGraphics, Marseille.
[10] Matthews, B.W. (1968) J. Mol. Biol. 33, 491–493.
[11] Brunger, A., Adams, P., Clore, G., DeLano, W., Gros, P., Grosse-Kunstleve, R., Jiang, J., Kuszewski, J., Nilges, M., Pannu, N., Read, R., Rice, L., Simonson, T. and Warren, G. (1998) Acta Crystallogr. D54, 905–921.
[12] Suh, S.W., Cascio, D., Chapman, M.S. and Eisenberg, D. (1987) J. Mol. Biol. 197, 363–365.
[13] Curmi, P., Cascio, D., Sweet, R.M., Eisenberg, D. and Schreuder, H. (1992) J. Biol. Chem. 267, 16980–16989.
[14] Newman, J. and Gutteridge, S. (1993) J. Biol. Chem. 268, 25876–25886.
[15] Zhang, K.Y.J., Cascio, D. and Eisenberg, D. (1994) Protein Sci. 3, 64–69.
[16] Newman, J. and Gutteridge, S. (1994) Structure 2, 495–502.
[17] Shibata, N., Inoue, T., Fukuhara, K., Nagara, Y., Kitagawa, R., Harada, S., Kasai, N., Uemura, K., Kato, K., Yokota, A. and Kai, Y. (1996) J. Biol. Chem. 271, 26449–26452.
[18] Andersson, I. (1996) J. Mol. Biol. 259, 160–174.
[19] Taylor, T.C., Fothergill, M.D. and Andersson, I. (1996) J. Biol. Chem. 271, 32894–32899.
[20] Taylor, T.C. and Andersson, I. (1997) Biochemistry 36, 4041–4046.
[21] Taylor, T.C. and Andersson, I. (1997b) J. Mol. Biol. 265, 432–444.
[22] Hansen, S., Vollan, V.B., Hough, E. and Andersen, K. (1999) J. Mol. Biol. 288, 609–621.
[23] Taylor, T.C., Backlund, A., Bjorhall, K., Spreitzer, R.J. and Andersson, I. (2001) J. Biol. Chem. 276, 48159–48164.
[24] Mizohata, E., Matsumura, H., Okano, Y., Kumei, M., Takuma, H., Onodera, J., Kato, K., Shibata, N., Inoue, T., Yokota, A. and Kai, Y. (2002) J. Mol. Biol. 316, 677–689.